

1
2
3
4
5
6
7
8
9
10
11
12
13
14
15
16
17
18
19
20
21
22
23
24

**Identification of residues controlling restriction versus enhancing activities of IFITM
proteins on the entry of human coronaviruses**

Xuesen Zhao^{1,2*}, Mohit Sehgal², Zhifei Hou¹, Junjun Cheng², Sainan Shu^{2,3}, Shuo Wu², Fang
Guo², Sylvain J. Le Marchand⁵, Hanxin Lin⁴, Jinhong Chang² and Ju-Tao Guo^{2*}

¹Beijing Ditan Hospital, Capital Medical University, Beijing 100015, China. ²Baruch S.
Blumberg Institute, Hepatitis B Foundation, 3805 Old Easton Road, Doylestown, PA 18902.
³Department of Pediatrics, Tongji Hospital, Tongji medical college, Huazhong University of
Science and Technology, Wuhan 430030, China. ⁴Department of Pathology and Laboratory
Medicine, Western University, 1151 Richmond Street, London, Ontario, Canada. ⁵Department of
Biology, Drexel University, Philadelphia, Pennsylvania, USA.

Running Title: IFITMs modulate human coronavirus entry

* Corresponding author's mailing address:

Xuesen Zhao, Beijing Ditan Hospital, Capital Medical University, Beijing, China. E-mail:

zhaoxuesen@ccmu.edu.cn

Ju-Tao Guo, Baruch S. Blumberg Institute, Doylestown, PA 18902. USA. E-mail: ju-

tao.guo@bblumberg.org

25 **ABSTRACT**

26 Interferon-induced transmembrane proteins (IFITM) are restriction factors that inhibit the
27 infectious entry of many enveloped RNA viruses. However, we demonstrated previously that
28 human IFITM2 and IFITM3 are essential host factors facilitating the entry of human coronavirus
29 (HCoV)-OC43. In a continuing effort to decipher the molecular mechanism underlying IFITM
30 differential modulation of HCoV entry, we investigated the role of structural motifs important for
31 IFITM protein post-translational modifications, intracellular trafficking and oligomerization in
32 modulating the entry of five HCoVs. We found that three distinct mutations in IFITM1 or
33 IFITM3 converted the host restriction factors to enhance the entry driven by the spike proteins of
34 severe acute respiratory syndrome coronavirus (SARS-CoV) and/or Middle East respiratory
35 syndrome coronavirus (MERS-CoV). First, substitution of IFITM3 tyrosine 20 with either
36 alanine or aspartic acid to mimic the unphosphorylated or phosphorylated IFITM3 reduced its
37 activity to inhibit the entry of HCoV-NL63 and 229E, but enhanced the entry of SARS-CoV and
38 MERS-CoV. Second, substitution of IFITM3 tyrosine 99 with either alanine or aspartic acid
39 reduced its activity to inhibit the entry of HCoV-NL63 and SARS-CoV, but promoted the entry
40 of MERS-CoV. Third, deletion of carboxyl-terminal 12 amino acid residues from IFITM1
41 enhanced the entry of MERS-CoV and HCoV-OC43. These findings suggest that these residues
42 and structural motifs of IFITM proteins are key determinants for modulating the entry of HCoVs,
43 most possibly through interaction with viral and/or host cellular components at the site of viral
44 entry to modulate the fusion of viral envelope and cellular membranes.

45 **Importance**

46

47 The differential effects of IFITM proteins on the entry of HCoVs that utilize divergent entry
48 pathways and membrane fusion mechanisms even when using the same receptor make the
49 HCoVs a valuable system for comparative investigation of the molecular mechanisms underlying
50 IFITM restriction or promotion of virus entry into host cells. Identification of three distinct
51 mutations that converted IFITM1 or IFITM3 from inhibitors to enhancers of MERS-CoV or
52 SARS-CoV spike protein mediated entry reveals key structural motifs or residues determining
53 the biological activities of IFITM proteins. These findings have thus paved a way for further
54 identification of viral and host factors that interact with those structural motifs of IFITM proteins
55 to differentially modulate the infectious entry of HCoVs.

56

57

INTRODUCTION

58

59 The interferon (IFN)-mediated innate immune response is the first line of defense against
60 virus infections in vertebrates (1, 2). IFNs execute antiviral activity by binding to their cognate
61 receptors on the cell surface to activate a signaling cascade leading to induction of hundreds of
62 IFN-stimulated genes (ISGs) (3, 4). Among those ISGs, IFN-induced transmembrane (IFITM)
63 proteins, including IFITM1, IFITM2 and IFITM3, are widely expressed and can be induced by
64 all three types of IFNs in many cell types. The IFITMs localize at the cell plasma membrane and
65 endocytic vesicles and restrict the entry of enveloped RNA viruses from nine viral families (5),
66 including some medically important human pathogens, such as influenza A virus (IAV), dengue
67 virus (DENV), West Nile virus, Zika virus, chikungunya virus, Ebola virus (EBOV), Rift Valley
68 fever virus, human immunodeficiency virus (HIV) and hepatitis C virus (3, 6-15).

69 Coronaviruses (CoVs) are a large family of enveloped, positive-stranded RNA viruses
70 with a broad host range and primarily cause respiratory or enteric diseases, but some of them
71 cause hepatitis, neurological disorders or cardiomyopathy (16, 17). Human coronaviruses (HCoV)
72 229E, OC43, NL63, and HKU1 circulate globally and cause mild upper respiratory tract
73 infections (18), but are occasionally associated with more severe lower respiratory tract diseases
74 in the elderly and immunocompromised patients (19). On the contrary, the recently emerging
75 HCoVs, such as severe acute respiratory syndrome coronavirus (SARS-CoV) and Middle East
76 respiratory syndrome coronavirus (MERS-CoV), cause severe diseases among infected
77 individuals (20, 21). Thus far, several groups have reported that IFITMs inhibited entry of
78 HCoV-229E, HCoV-NL63, SARS-CoV and MERS-CoV into their host cells with varying
79 efficiency (8, 22, 23).

4

80 Concerning the molecular mechanism underlying IFITM restriction of virus entry, the
81 currently favored hypothesis postulates that existence of IFITM proteins in the endocytic
82 membranes either alters the membrane curvature or fluidity to make the endosomal membrane
83 rigid and harder to fuse with viral envelopes (24, 25) (26-28). However, several recent findings
84 challenge this hypothesis. First, human IFITM2 and IFITM3 efficiently enhance the infectious
85 entry of HCoV-OC43 *via* a post receptor binding/endocytosis mechanism (29). Second, mutation
86 of the SVKS motif in the CD225 domain required for IFITM1 to inhibit HIV-1 entry and
87 IFITM3 to restrict IAV and dengue virus infection (24, 30) enhances Lloviu virus (LLOV)
88 glycoprotein-mediated entry (Fig. 11) (31). Third, human IFITM proteins are required for the
89 formation of human cytomegalovirus virion assembly complex (VAC) and infectious virion
90 secretion (32). The VAC is a perinuclear membrane structure where the vesicles with endosomal
91 markers occupy the central area and the vesicles with the Golgi markers are wrapped around it to
92 form a circle (33). It is possible that IFITMs modulate endosomal trafficking/fusion during the
93 VAC formation. All those findings strongly suggest that the IFITM-induced membrane curvature
94 and/or fluidity alterations may not always make the endocytic membranes too “rigid” to fuse, but
95 at least under certain condition, may facilitate membrane fusion.

96 In order to further understand the molecular mechanism underlying the differential
97 modulation of IFITM proteins on HCoV entry, we set out to identify structural motifs important
98 for IFITM protein post-translational modifications, intracellular trafficking and oligomerization
99 in modulating the entry of five HCoVs. We found that although both SARS-CoV and NL63 use
100 angiotensin-converting enzyme 2 (ACE2) as their entry receptor, IFITMs differentially modulate
101 the entry of these two viruses. We also found that three distinct mutations in IFITM1 or IFITM3
102 converted the host restriction factors to enhancers of SARS-CoV and/or MERS-CoV entry.

103 These findings imply that restriction or promotion of a virus entry by an IFITM may rely on its
104 fine-tuned interaction with viral and host cellular factors *via* those structural motifs at the site of
105 viral envelope and cellular membrane fusion. Moreover, post-translation modification of those
106 structural motifs by host cellular factors may alter IFITM interaction with the components of
107 viral entry machinery and consequentially change its potency and/or nature of modulating the
108 entry of a virus.

109

110

RESULTS

111

112 **Host cellular factors other than viral receptors have a strong impact on antiviral activity of**
113 **IFITM proteins.** Viral envelope proteins and cellular receptors are the major players of virus
114 entry into their host cells. It is conceivable that IFITM interaction with viral envelope and/or
115 cellular receptors may play an important role in restriction of virus entry. Angiotensin-converting
116 enzyme 2 (ACE2), as the common receptor for both SARS-CoV and NL63, provides a unique
117 opportunity to investigate the role of viral receptor in IFITM modulation of HCoV entry (34).
118 Accordingly, we examined the effects of three human IFITMs proteins on the entry of four
119 HCoVs, with lassa fever virus (LASV) and influenza A virus (IAV) as negative and positive
120 controls, in HEK293 and hepatoma cell line Huh7.5 that express detectable and undetectable
121 basal levels of IFITMs, respectively (29) (Fig. 1). As anticipated, expression of any of the three
122 IFITMs in either HEK293 or Huh7.5 cells did not inhibit the infection of lentiviral particles
123 pseudotyped with the envelope proteins of lassa fever virus (LASVpp) (Figs. 1B and 1C).
124 However, all the three IFITMs significantly inhibited the infection of lentiviral particles
125 pseudotyped with IAV hemagglutinin 1 (H1) and neuraminidase 1 (N1) (IAVpp), Spike protein

126 (S) of HCoV-229E (229Epp), HCoV-NL63 (NL63pp), SARS-CoV (SARSpp) and MERS-CoV
127 (MERSpp) in both HEK293 (Fig.1B) and Huh7.5 cells (Fig. 1C). However, comparing the extent
128 of IFITM inhibition between the two cell lines (Figs. 1B and C), IFITM2 and IFITM3 inhibition
129 of IAVpp infection was 4- and 20-fold more potent, respectively, in HEK293 cells than that in
130 Huh7.5 cells. On the contrary, IFITM2 and IFITM3 more efficiently inhibited entry of all four
131 HCoVpp, particularly for MERSpp and 229Epp, in Huh7.5 cells. The steady state levels of
132 IFITM1 were lower than that of IFITM2 and IFITM3 in both HEK293 and Huh7.5 cells, which
133 may, at least in part, explain its lower activity to inhibit the infection of all the tested
134 pseudoviruses, except for 229Epp. Interestingly, IFITM1 more potently inhibited 229Epp
135 infection than IFITM2/3 in HEK293 cells, but was less effective in Huh7.5 cells. While the viral
136 envelope proteins are obviously the primary determinants of the potency of IFITMs to restrict
137 virus entry, the more potent inhibition by all three IFITMs on the infection of NL63pp than that
138 of SARSpp suggests that host cellular factors other than viral receptors have a strong impact on
139 antiviral activity of IFITMs.

140

141 **Substitution of Y20 in IFITM3 enhances SARS-CoV and MERS-CoV entry.** We next aimed
142 at identifying IFITM structural motifs that control the modulation of HCoV entry. IFITM
143 proteins contain a conserved CD225 domain flanked by sequence-divergent N- and C-terminal
144 variable regions (5). The N-terminal 21 amino acid residues unique to IFITM2 or 3 has been
145 demonstrated to be important for IFITM3 to inhibit IAV infection in cultured cells and *in vivo* in
146 humans (35-38). It has been shown recently that the N-terminal region of IFITM3 contains a 20-
147 YEML-23 tetrapeptide that is consistent with the canonical Yxx Φ endocytic sorting signal (x can
148 be any amino acid, Φ denotes Val, Leu, or Ile) (39-41). Furthermore, the Y20 can be

149 phosphorylated by tyrosine kinase Fyn, which regulates the IFITM3 trafficking and metabolism
150 (42). We thus investigated how the phosphorylation of IFITM3 at Y20 may regulate its function
151 of modulating HCoV entry. The results showed that compared to wild-type IFITM3, substitution
152 of Y20 with alanine (A) and aspartic acid (D) or glutamic acid (E) to mimic the non-
153 phosphorylated (Y20A) or phosphorylated (Y20E or Y20D) IFITM3, respectively, did not alter
154 the steady-state levels of expression (Figs. 2A and F) and activity to enhance the entry of HCoV-
155 OC43 in both HEK293 and Huh7.5 cells (Figs. 2B and G). However, the mutant IFITM3
156 proteins showed significantly reduced activity to inhibit NL63pp and 229Epp infection (Figs. 2C,
157 D, H and I). On the contrary, mutant IFITM3 proteins enhanced the infection of SARSpp and
158 MERSpp in both cell lines (Figs. 2C, E, H and J). Consistent with previous reports (39, 40),
159 wild-type IFITM3 was accumulated in the perinuclear region and primarily co-localized with
160 Rab9, a later endosome marker (43) (Fig. 3A). In contrast, IFITM3 proteins bearing Y20A or
161 Y20D mutation were primarily accumulated in the regions closed to the plasma membrane (Fig.
162 3B and 3C). These results indicate that Y20 is critical for endocytic sorting, which is regulated
163 by tyrosine phosphorylation.

164 In order to investigate whether the enhanced infection of SARSpp and MERSpp by the
165 mutant IFITM3 proteins is due to the induction of membrane fusion on the plasma membrane,
166 we examined the effect of endosomal pH on HCoVpp infection of Huh7.5 cells expressing wild-
167 type or Y20A IFITM3 (Fig. 4). As shown in Figs. 4A, among the five tested HCoVpp, MERSpp
168 and NL63pp infection were less sensitive to NH₄Cl treatment that elevates endosomal pH,
169 suggesting that the membrane fusion for those two viruses may occur in early endosomal
170 compartments. Interestingly, IFITM3 Y20A-enhanced SARSpp and MERSpp infection were
171 efficiently inhibited by NH₄Cl treatment in a concentration-dependent manner (Figs. 4B and C).

172 The results thus suggest that although Y20 mutant IFITM3 proteins are primarily accumulated in
173 the plasma membrane regions, the enhanced infection of SARSpp and MERSpp still occurs in
174 low pH endosomal compartments.

175

176 **Substitution of Y99 in IFITM3 enhances MERS-CoV entry.** In addition to Y20, Y99 had
177 been shown to be phosphorylated in cells by mass spectrometry analysis and play a role in
178 restricting the infectious entry of IAV, but not dengue virus (24). Therefore, we performed
179 phosphomimetic analysis on this amino acid residue. As shown in Fig. 5A, the Y99A or Y99D
180 mutant IFITM3 was expressed to a level similar to that of wild-type IFITM3. Compared with
181 wild-type IFITM3, Y99A or Y99D mutants had a slightly increased activity to enhance OC43pp
182 infection, but significantly reduced activity to inhibit the infection of SARSpp, NL63pp, IAVpp
183 and VSVpp (Figs. 5B to E). Intriguingly, both Y99A and Y99D IFITM3 enhanced MERSpp
184 infection by approximately 10-fold (Fig. 5F). The results imply that Y99 plays a critical role in
185 IFITM3 modulation of the entry of different HCoVs.

186

187 **Oligomerization of IFITM3 is essential for its suppression of the entry of HCoVs, except**
188 **for NL63.** In addition to phosphorylation, the function of IFITM proteins is regulated by
189 cysteine palmitoylation (44, 45), ubiquitination (46, 47) as well as homo- and hetero-
190 oligomerization (24, 29). To investigate the role of these post-translational modifications in
191 IFITM3 inhibition of HCoV entry, HEK293 cell lines inducibly expressing wild-type or mutant
192 IFITM3 proteins bearing mutations that preclude the cysteine palmitoylation or ubiquitination
193 were established. Specifically, the conserved cysteine residues C71 and C72 or one additional
194 cysteine C105, that are critical for IFITM3 palmitoylation, were substituted with alanine to yield

195 two mutants, IFITM3/2CA and IFITM3/3CA, respectively. As shown in Figs. 6A and 6B, the
196 mutations had minimal impacts on protein expression, but completely abolished activity to
197 restrict the infection of all the five pseudoviruses sensitive to IFITM3. However, IFITM3/4KA,
198 that was generated by substitution of K24, K83, K88 and K104 with alanines, accumulated in a
199 significantly reduced level in cells and failed to inhibit the infection of all the pseudoviruses
200 examined. Moreover, IFITM3 containing F75A and F78A mutations (IFITM3/2FA), that disrupt
201 its oligomerization (29), completely lost ability to inhibit the infection of SARSpp, 229Epp,
202 MERSpp, and IAVpp, but could still significantly inhibit the infection of NL63pp, despite
203 reduced activity (Fig. 6B). The results thus suggest that unlike other viruses (24, 29), suppression
204 of NL63 spike protein triggered membrane fusion does not absolutely require the
205 oligomerization of IFITM3.

206

207 **C-terminal domain of IFITM1 differentially regulates the entry of HCoV.** We showed
208 previously that sequential truncation of the C-terminal 18 amino acid residues from IFITM1 did
209 not apparently affect its activity to inhibit the infection of IAVpp, but converted the antiviral
210 protein to an increasingly potent enhancer of OC43pp infection (29). In our efforts toward
211 further dissecting the role of C-terminal domain (CTD) in IFITM1 modulation of HCoV entry,
212 we found that deletion of C-terminal 3, 6 or 9 amino acids did not apparently affect the activity
213 of IFITM1 to inhibit the infection of SARSpp, but further deletion of C-terminal 12, 15 or 18
214 amino acids significantly compromised or abolished the ability of IFITM1 to inhibit the infection
215 of SARSpp (Fig. 7B). In contrast, deletion of C-terminal 3, 6 and 9 amino acids enhanced the
216 activity of IFITM1 to inhibit the infection of NL63pp by 5, 10 and 3 fold, respectively. However,
217 further truncation of the C-terminal 12, 15 or 18 amino acids abolished the enhanced inhibitory

218 effect on NL63pp infection (Fig. 7B). Interestingly, sequential truncation of the CTD gradually
219 attenuated and ultimately abolished the activity of IFITM1 to inhibit 229Epp infection (Fig. 7C).
220 On the contrary, sequential truncation of C-terminal 12 amino acids gradually increased its
221 activity to enhance MERSpp infection, but further deletion of C-terminal 15 or 18 amino acids
222 reduced its activity to enhance MERSpp infection (Fig. 7D).

223 To rule out the potential interference of endogenous IFITM proteins on mutant IFITM1
224 in HEK 293 cells (29), we further confirmed the observation in Huh7.5 cells that express
225 undetectable endogenous IFITM proteins. Four Huh7.5 cell lines were established by
226 transduction with empty retroviral vector or retroviral vector expressing wild-type IFITM1,
227 IFITM1/TC6 or IFITM1/TC18 protein. Consistent with the observations made in HEK293 cells,
228 deletion of C-terminal 18, but not 6, amino acids significantly compromised IFITM1 to suppress
229 SARSpp infection and deletion of C-terminal 6, but not 18, amino acids significantly enhanced
230 activity to inhibit NL63pp infection (Fig. 8B). In agreement with the results obtained with
231 NL63pp infection, we also observed that deletion of C-terminal 6, but not 18, amino acids
232 significantly increased the ability of IFITM1 to inhibit the infection of HCoV-NL63, as judged
233 by significant reduction in infected cell percentage and intracellular viral RNA (Figs. 8C and D).

234 Taken together, the results suggest that two partially overlapped functional motifs exist in
235 the CTD of IFITM1. While its C-terminal 9 to 12 amino acid residues contain a motif that down-
236 regulates the antiviral activity against HCoV-NL63 and suppresses the enhancing activity to
237 MERS-CoV infection, the motif located in the N-terminal 9 amino acid residues of the CTD is
238 important for IFITM1 to suppress SARS-CoV and HCoV-229E entry.

239 To investigate the molecular mechanisms underlying the differential modulation of
240 HCoV entry by the CTD, we examined the subcellular localization of wild-type and mutant

241 IFITM1 proteins. As shown in Fig.9, similar to wild-type IFITM1, IFITM1/TC6 and
242 IFITM1/TC18 are primarily accumulated in regions close to or at the plasma membrane.
243 However, a modestly increased intracellular localization of both IFITM1/TC6 and IFITM1/TC18
244 is evident. Specifically, IFITM1/TC6 tends to more frequently co-localize with Rab5 and Rab9,
245 whereas IFITM1/TC18 is more frequently co-localized with EEA1, an early endosomal marker
246 (48), and Rab9, a later endosomal marker. Moreover, as shown in Fig. 10, compared to wild-type
247 IFITM1, IFITM1/TC6, but not IFITM1/C18, demonstrated reduced mono- and di-ubiquitination.
248 As anticipated, substitution of four residues of lysine in IFITM3 (IFITM3/4KA) completely
249 abolished ubiquitination. The results thus indicate that the CTD of IFITM1 contains structural
250 motif(s) that regulates its subcellular trafficking and ubiquitination, which may consequentially
251 affect its activity to modulate the entry of HCoV.

252

253

DISCUSSION

254

255 In spite of the relatively broad spectrum of antiviral activities, IFITM proteins do not
256 restrict the infection of MLV, Sendai virus and several members of *Arenaviridae* family as well
257 as all the DNA viruses tested thus far (6, 8, 49, 50). The molecular determinants that control the
258 viral specificity and potency of IFITMs remain to be fully understood. Because viral envelope
259 proteins and cellular receptors are the two major players of viral membrane fusion, it is plausible
260 to consider that modulating the interaction between viral envelope proteins and cellular receptors
261 might be the key mechanism of IFITM restriction of virus entry. Indeed, it was reported recently
262 that IFITM sensitivity of HIV-1 strains is determined by the co-receptor usage of viral envelope
263 glycoproteins (51, 52). However, the difference in the potency and requirement of IFITM

264 oligomerization in inhibition of SARSpp and NL63pp infection (Figs. 1 and 6) and particularly,
265 the results that IFITM3/Y20 phosphomimetic mutations only enhanced the infection of SARSpp,
266 but not NL63pp (Fig. 2) strongly suggest that IFITM interaction with viral and host cellular
267 factors, other than viral receptors, such as ACE2, play a critical role in IFITM modulation of
268 virus entry. Furthermore, our findings that IFITM2 and IFITM3 promoted HCoV-OC43
269 infection, and three distinct mutations converted IFITM1 or IFITM3 from inhibitors to enhancers
270 of SARS-CoV and/or MERS-CoV spike protein-mediated entry challenge the “rigid” membrane
271 hypothesis and suggest that IFITM proteins may also promote the membrane fusion, under
272 selected conditions, to facilitate virus entry.

273 Based on those new findings, we hypothesize that depending on the fine-tuned interaction
274 with the entry machinery of a given virus, which consists of viral envelope components as well
275 as viral receptors and other host entry factors at the site of membrane fusion, IFITM proteins can
276 either promote or arrest the fusion between viral envelope and endosomal membranes (29). It is
277 possible that the three structural motifs identified herein mediate interactions with key host
278 factors to determine either to arrest or to enhance the membrane fusion. Along this line, recent
279 studies revealed that zinc metallopeptidase STE24 forms complexes with IFITM proteins and is
280 required for IFITMs to inhibit the entry of many different viruses (53). In addition, the sensitivity
281 of IAVs to IFITM3 appears to depend on the pH value at which the viral HA undergoes a
282 conformational transition and mediates membrane fusion (54). More interestingly, IFITM
283 expression promotes the uptake of avian sarcoma leukosis virus (ASLV) and the acidification of
284 endosomal compartments, resulting in an accelerated membrane fusion when driven by the
285 glycosylphosphatidylinositol-anchored, but not by the transmembrane isoform of the ASLV
286 receptor (55). These recent findings clearly highlight the regulation of multiple viral and host

287 cellular components on IFITM modulation of the fusion between viral envelope and endosomal
288 membranes during viral infections.

289 Our new hypothesis predicts that in order to modulate virus entry, IFITM proteins ought
290 to be at the site of viral membrane fusion (26-28). Indeed, previous studies demonstrated in a
291 variety of virus infection systems that localization at the subcellular compartment where a virus
292 enters into the cytoplasm is important for the IFITM protein to inhibit its infectious entry (5). For
293 instance, disruption of the canonical endocytic signal in IFITM3 by Y20A/E/D mutations
294 resulted in its plasma membrane accumulation (Fig. 11). As a consequence, the mutant IFITM3
295 demonstrated a reduced antiviral activity against IAV that enter cells by fusion with lysosomal
296 membrane (39-41), but enhanced the activity to restrict the infection of parainfluenza virus 3, a
297 virus that enters cells by fusion with the plasma membrane (56). However, the subcellular
298 localization of IFITM proteins is not always strictly correlated with antiviral activity. For
299 example, while IFITM3 Y99A mutation does not apparently alter the subcellular localization, the
300 mutation significantly compromises the antiviral activity of IFITM3 against IAV, but not dengue
301 virus (24). In this study, we further demonstrated that although Y20A mutant IFITM3 was
302 predominantly accumulated in the plasma membrane regions, its enhanced infection of SARSpp,
303 MERSpp and OC43pp was still low pH dependent (Fig. 4) (29), suggesting that the enhanced
304 entry of those viruses still occurs in low pH intracellular endosomal compartments. The apparent
305 contradiction between the subcellular localization of the mutant IFITM3 proteins and site of
306 membrane fusion implies that a small fraction of the mutant IFITM3 might still traffic to the sites
307 where the viral spike protein-induced membrane fusion occurs. In addition, phosphomimetic
308 analyses suggest that Y20 or Y99 tyrosine phosphorylation regulates the metabolism, trafficking
309 and biological function of IFITM3.

310 In addition to tyrosine phosphorylation, IFITM3 can also be post-translationally modified
311 at more than 8 different amino acid residues with at least three different types of modifications,
312 including palmitoylation, ubiquitination and methylation (42, 44-47, 57). Our mutagenesis
313 studies showed that both palmitoylation and ubiquitination are absolutely required for IFITM3 to
314 modulate the entry of all the tested HCoV (Fig. 6). Moreover, oligomerization of IFITM
315 proteins has been demonstrated to be essential for their restriction of IAV and dengue virus
316 infection as well as enhancement of HCoV-OC43 infection (24, 29). Interestingly, hetero-
317 oligomerization between IFITM1 and IFITM3, that inhibits and enhances HCoV-OC43 infection,
318 respectively, antagonize each other's functions (29). In this study, we further revealed that
319 IFITM3 bearing F75A and F78A mutations that disrupt its oligomerization completely lost its
320 ability to inhibit the infection of SARSpp, 229Epp and MERSpp, but still partially inhibited
321 NL63pp infection (Figs. 6 and 11). While the results reinforce the notion that oligomerization is
322 important for IFITMs to modulate the entry of many viruses, NL63 appears to be an exception.

323 It was reported previously that the CTD of IFITM1, illustrated in Fig. 11, plays an
324 important role in modulating the entry of HCoV-OC43 (29), HIV1 (58), jaagsiekte sheep
325 retrovirus and 10A1 amphotropic murine leukemia virus (59). In this study, we showed that the
326 CTD of IFITM1 plays distinct roles in modulating the entry of different HCoVs. It appears that
327 the CTD contains two overlapping functional motifs. While the C-terminal 9 and 12 amino acid
328 residues negatively regulate IFITM restriction of HCoV-NL63 entry and enhancement of MERS-
329 COV infection, the motif located in the N-terminal 9 amino acid residues of the CTD is
330 important for IFITM1 to suppress SARS-CoV and HCoV-229E entry. In search for the
331 underlined mechanism, a study identified a dibasic ¹²²KRxx¹²⁵ motif at the C-terminus of
332 IFITM1 regulates IFITM1 intracellular trafficking with reduced localization in LAMP1-positive

333 lysosomes, but increased levels in CD63-positive multivesicular bodies (59). IFITM1 binds to
334 cellular adaptor protein complex 3 (AP-3), an association that is lost when the dibasic motif is
335 altered (59). However, we found that partial or complete deletion of the CTD does not
336 dramatically alter its subcellular distribution (Fig. 9). Instead, deletion of 6, but not 18 amino
337 acid residues from the C-terminus reduced IFITM1 ubiquitination (Fig. 10). The results
338 collectively indicate that the CTD is a key regulator of IFITM function. However, its effects on
339 the entry of different viruses imply a versatile function of the CTD. Further investigation into the
340 structure, post-translational modification and membrane topology of the CTD as well as
341 identification of the cellular and/or viral proteins interacting with the CTD will shed light on the
342 mechanism by which the CTD regulates the function of IFITM1.

343 In summary, we demonstrated in this study that in addition to viral envelope proteins and
344 cellular receptors, IFITM protein oligomerization, post-translational modification and
345 intracellular trafficking, which can be regulated by host cellular pathobiological cues, play
346 critical roles in determining the extent and nature of IFITMs to modulate the entry of HCoVs.
347 More importantly, identification of the three structural motifs that reverse the function of
348 IFITM1 and IFITM3 on virus entry paves the way for uncovering viral and host factors that
349 interact with those structural motifs to differentially modulate the infectious entry of HCoVs and
350 other viruses (53).

351

352

MATERIALS AND METHODS

353

354 **Cell lines, viruses, and antibodies.** LLC-MK2 cells were cultured in minimal essential medium
355 (MEM), which was prepared by mixing Hanks MEM (Invitrogen, Cat. No. 11575-032) and
356 Earle's MEM (Invitrogen, Cat. No. 11095-080) in 2:1 ratio, and supplemented with 10% heat-

357 inactivated fetal bovine serum (FBS) (Invitrogen). Huh7.5 cells were cultured with Dulbecco's
358 modified Eagle's medium (DMEM) [Corning] supplemented with 10% FBS, 1x nonessential
359 amino acids (Invitrogen) and 2 mM L-glutamine (Invitrogen). Human colon cancer cell line
360 HCT-8 was grown in RPMI-1640 medium (ATCC, Cat. No. 30-2001) supplemented with 10%
361 FBS. GP2-293 and Lenti-X 293T cell Lines were purchased from Clontech and cultured in
362 DMEM supplemented with 10% FBS and 1 mM Sodium pyruvate (Invitrogen). FLP-IN T Rex
363 293 cells were purchased from Invitrogen and maintained in DMEM supplemented with 10%
364 FBS, 10 µg/ml blasticidin (Invitrogen) and 100 µg/ml Zeocin (Invivogen) (60). HCoV-NL63 was
365 purchased from ATCC through BEI Resource (Cat. No. NR470) and amplified in LLC-MK2
366 cells. Virus titers were determined by a plaque assay (29). Monoclonal antibody against FLAG
367 tag (anti-FLAG M2), rabbit anti-FLAG polyclonal antibody and β-actin antibody were purchased
368 from Sigma (Cat. No. F1804, F7425 and A2228, respectively). A mouse monoclonal antibody
369 against HCoV-NL63 nucleocapsid (N) protein was purchased from Ingenansa, Spain (Cat. No.
370 M.30.HCo.I2D4).

371

372 **Plasmids.** pcDNA5/FRT-derived plasmids expressing chloramphenicol acetyl transferase (CAT),
373 N-terminally FLAG-tagged human IFITM1, IFITM2 and IFITM3 as well as C-terminally
374 truncated IFITM1 mutants were reported previously (7, 60, 61) (29). Plasmids expressing N-
375 terminally FLAG-tagged mutant IFITM3 proteins with point mutations were constructed by
376 overlap extension PCR (60). All resulting plasmids were sequenced to verify the desired
377 mutation(s). N-terminally FLAG-tagged human IFITM1, IFITM2 and IFITM3 and their mutants
378 were also cloned into pQCXIP vector (Clontech) between the NotI and BamHI sites (29).

379 Plasmids expressing HCoV-OC43 spike (S) and HE proteins, VSV G protein, H1N1 IAV
380 (A/WSN/33) hemagglutinin (HA) and neuraminidase (NA), Ebola virus (EBOV) GP protein,
381 LASV GP protein, murine leukemia virus (MLV) envelope protein, HCoV-NL63 and SARS-
382 CoV spike protein were described previously (62, 63). MERS-CoV spike gene (GenBank
383 accession number AFS88936) was synthesized by GeneScript, cloned into pCAGGS vector, and
384 confirmed by DNA sequence analyses. Plasmid pNL4-3.Luc.R^E was obtained through the NIH
385 AIDS Research and Reference Reagent Program (64, 65). Angiotensin I converting enzyme 2
386 (ACE2), aminopeptidase N (APN), and dipeptidyl peptidase-4 (DPP4) cDNA clones were
387 obtained from Origene, and cloned into a pcDNA3 vector (Invitrogen) to yield plasmid pcDNA3
388 /ACE2, pcDNA3 /APN and pcDNA3/DDP4, respectively (66).

389

390 **Package of pseudotyped retroviral particles.** The various viral envelope protein pseudotyped
391 lentiviruses bearing luciferase reporter gene as well as VSV G protein pseudotyped retroviruses
392 expressing wild-type and mutant IFITM mutant proteins were packaged as reported previously
393 (66, 67). Each pseudotype was titrated by infection of cells with a serial dilution of pseudotype
394 preparations. The modulation of IFITM on the transduction of a given pseudotype was
395 determined with a titrated amount of pseudotypes that yield luciferase signal between 10,000 to
396 1,000,000 light units per well of 96-well plates. For a given pseudotype, the input of pseudoviral
397 particles is consistent across all the experiments.

398

399

400 **Establishment of cell lines stably expressing wild-type and mutant IFITM proteins.** Huh7.5
401 cells in each well of 6-well plates were incubated with 2 ml of Opti-MEM medium containing

402 pseudotyped retroviruses and centrifuged at 20 °C for 30 minutes at 4,000×g. Forty-eight h post
403 transduction, cells were cultured with media containing 2 µg/ml of puromycin for two weeks.
404 The antibiotic resistant cells were pooled and expanded into cell lines stably expressing human
405 wild-type or mutant IFITM proteins (66). FLP-IN T Rex 293-derived cell lines expressing
406 mutant IFITM proteins in a tetracycline (tet) inducible manner were established as previously
407 described (7, 60).

408

409 **Western blot assay.** Cell monolayers were washed once with Phosphate Buffered Saline (PBS)
410 and lysed with 1× Laemmli buffer. An aliquot of cell lysate was separated on NuPAGE® Novex
411 4-12% Bis-Tris Gel (Invitrogen) and electrophoretically transferred onto a nitrocellulose
412 membrane (Invitrogen). The membranes were blocked with PBS containing 5% nonfat dry milk
413 and probed with the desired antibody. The bound antibodies were visualized with IRDye
414 secondary antibodies and imaging with LI-COR Odyssey system (LI-COR Biotechnology).

415

416 **Real-time RT-PCR.** Total cellular RNA was extracted by using TRIzol reagent (Invitrogen) and
417 reverse transcribed by using SuperScript III (Invitrogen). Quantitative PCR (qPCR) reaction was
418 performed as previously described on LightCycler 480II (Roche) with modified forward primer
419 [5'-AAA CCT CGT TGG AAG CGT GTTC-3'] and reverse primer [5'- CTG TGG AAA ACC
420 TTT GGC ATC-3'] under the following conditions: denature at 95 °C for 10 min and 45 cycles
421 of amplification (15 s at 95 °C and 1 min at 60 °C). The PCR reaction amplifies a fragment of
422 HCoV-NL63 N gene (GenBank Gene ID: 2943504).

423

424 **Luciferase assay.** T REX 293-derived IFITM-expressing cell lines were seeded into 96-well
425 plates with black wall and clear bottom and transfected with plasmids encoding ACE2, APN, or
426 DPP4 to express viral receptors. For Huh7.5-derived IFITM-expressing cell lines, cells were
427 seeded into black wall 96-well plates. Cells were infected at 24 h post transfection or seeding
428 with desired pseudotyped lentiviral particles for 2 h, and then replenished with fresh media. Two
429 days post infection, the media were removed and cells were lysed with 20 μ l/well of cell lysis
430 buffer (Promega) for 15 min, followed by adding 50 μ l/well of luciferase substrate (Promega).
431 The firefly luciferase activities were measured by luminometry in a TopCounter (Perkin Elmer)
432 (66).

433

434 **Immunofluorescence** To visualize HCoV-NL63 infected cells, the infected cultures were fixed
435 with 4% paraformaldehyde for 20 min. After permeabilization with 0.1% Triton X-100, cells
436 were stained with a monoclonal antibody recognizing HCoV-NL63 N protein (Ingenansa, Spain,
437 Cat. No. M.30.HCo.I2D4). Bound antibodies were visualized by using Alexa Fluor 488-labeled
438 goat anti-mouse IgG (Abcam, Cat. No. ab150113). Cell nuclei were counterstained with 4',6-
439 Diamidine-2'-phenylindole dihydrochloride (DAPI).

440 For determination of mutant IFITM1 or IFITM3 subcellular localization, T REX 293-
441 derived cell lines inducibly expressing mutant IFITM proteins were fixed and permeabilized as
442 described above. The cells were then stained with anti-FLAG monoclonal antibody together with
443 a rabbit derived polyclonal antibody against EEA1 (Cell Signaling, Cat. No. 2411), Rab5 (Cell
444 Signaling, Cat. No. 2143) or Rab9 (Cell Signaling, Cat. No. D52G8), respectively. The bound
445 antibodies were visualized using Alexa Fluor 594-labeled goat anti-mouse IgG (red) and Alex
446 Fluor 488-labeled goat anti-rabbit IgG (green). Cell nuclei were counterstained with DAPI.

447 Images were sequentially acquired on a FV1000 confocal microscope (Olympus) with a
448 PlanApoN 60×/1.42 N objective (Olympus). Pinhole size was adjusted to 1 airy unit. Optimal
449 diffraction-limited spatial resolution was obtained using a pixel size of 82 nm /pixel. DAPI was
450 excited at 405 nm and its fluorescence emission collected between 430 nm and 470 nm. Alexa
451 Fluor 488 was excited at 488nm and its fluorescence emission collected between 505 and 525
452 nm. Alexa Fluor 594 was excited at 543nm and its fluorescence emission collected between 560
453 and 660 nm. Negative controls were performed to make sure that there were no significant
454 spectral bleed-through artifacts between channels.

455

456 **TCID₅₀.** Confluent LLC-MK2 cells cultured in 96-well plates were infected with 200 µl of
457 OPTI-MEM containing a serial 10-fold dilution of viral stock for 2 h at 33 °C. Cells were then
458 cultured at 33 °C with MEM with 2.5% FBS for 6 days. The cells of each well with cytopathic
459 effect (CPE) were visualized and counted under microscope. The TCID₅₀ of virus stock was
460 measured and converted to pfu/ml (68).

461

462 **Immunoprecipitation** To detect ubiquitination of IFITM protein and its mutants, IP-western
463 blot was performed as reported previously (29, 44). Briefly, 293T cells were transfected with
464 plasmids expressing FLAG-tagged IFITM1, IFITM3 and their mutants, respectively. Cells were
465 lysed at 48 h post transfection with lysis buffer containing 50 mM Tris-HCl (pH 7.4), 150 mM
466 NaCl, 1 mM EDTA, and 1% Triton X-100 and protease inhibitors (Roche) and
467 immunoprecipitated with a monoclonal antibody against FLAG epitope followed by incubation
468 with Protein A/G-Agarose beads (PIERCE) and washing with TBS buffer. The
469 immunocomplexes were resolved in a NuPAGE® Novex 4-12% Bis-Tris Gel in MES buffer

470 (Invitrogen) and transferred on to a PVDF membrane. The membrane was probed with rabbit
471 polyclonal antibody against Flag epitope (Sigma, Cat. No. F7425) or anti-ubiquitin rabbit
472 polyclonal antibody (Proteintech, Cat. No. 10201-2-AP). The bound antibodies were visualized
473 with IRDye secondary antibodies and imaged with LI-COR Odyssey system (LI-COR
474 Biotechnology).

475

476 **ACKNOWLEDGEMENTS**

477 This work was supported by grants from the National Institutes of Health, USA (AI113267),
478 National Natural Science Foundation of China (81571976) and The Commonwealth of
479 Pennsylvania through the Hepatitis B Foundation.

480

REFERENCES

481

- 482 1. **Cullen BR, Cherry S, tenOever BR.** 2013. Is RNA interference a physiologically
483 relevant innate antiviral immune response in mammals? *Cell Host Microbe* **14**:374-378.
- 484 2. **Chang J, Block TM, Guo JT.** 2012. The innate immune response to hepatitis B virus
485 infection: implications for pathogenesis and therapy. *Antiviral Res* **96**:405-413.
- 486 3. **Diamond MS, Farzan M.** 2013. The broad-spectrum antiviral functions of IFIT and
487 IFITM proteins. *Nat Rev Immunol* **13**:46-57.
- 488 4. **Bailey CC, Zhong G, Huang IC, Farzan M.** 2014. IFITM-Family Proteins: The Cell's
489 First Line of Antiviral Defense. *Annual review of virology* **1**:261-283.
- 490 5. **Perreira JM, Chin CR, Feeley EM, Brass AL.** 2013. IFITMs restrict the replication of
491 multiple pathogenic viruses. *J Mol Biol* **425**:4937-4955.
- 492 6. **Brass AL, Huang IC, Benita Y, John SP, Krishnan MN, Feeley EM, Ryan BJ,
493 Weyer JL, van der Weyden L, Fikrig E, Adams DJ, Xavier RJ, Farzan M, Elledge
494 SJ.** 2009. The IFITM proteins mediate cellular resistance to influenza A H1N1 virus,
495 West Nile virus, and dengue virus. *Cell* **139**:1243-1254.
- 496 7. **Jiang D, Weidner JM, Qing M, Pan XB, Guo H, Xu C, Zhang X, Birk A, Chang J,
497 Shi PY, Block TM, Guo JT.** 2010. Identification of five interferon-induced cellular
498 proteins that inhibit west nile virus and dengue virus infections. *J Virol* **84**:8332-8341.
- 499 8. **Huang IC, Bailey CC, Weyer JL, Radoshitzky SR, Becker MM, Chiang JJ, Brass
500 AL, Ahmed AA, Chi X, Dong L, Longobardi LE, Boltz D, Kuhn JH, Elledge SJ,
501 Bavari S, Denison MR, Choe H, Farzan M.** 2011. Distinct patterns of IFITM-mediated
502 restriction of filoviruses, SARS coronavirus, and influenza A virus. *PLoS Pathog*
503 **7**:e1001258.
- 504 9. **Mudhasani R, Tran JP, Retterer C, Radoshitzky SR, Kota KP, Altamura LA, Smith
505 JM, Packard BZ, Kuhn JH, Costantino J, Garrison AR, Schmaljohn CS, Huang IC,
506 Farzan M, Bavari S.** 2013. IFITM-2 and IFITM-3 but not IFITM-1 restrict Rift Valley
507 fever virus. *J Virol* **87**:8451-8464.
- 508 10. **Anafu AA, Bowen CH, Chin CR, Brass AL, Holm GH.** 2013. Interferon-inducible
509 transmembrane protein 3 (IFITM3) restricts reovirus cell entry. *J Biol Chem* **288**:17261-
510 17271.
- 511 11. **Wilkins C, Woodward J, Lau DT, Barnes A, Joyce M, McFarlane N, McKeating JA,
512 Tyrrell DL, Gale M, Jr.** 2013. IFITM1 is a tight junction protein that inhibits hepatitis C
513 virus entry. *Hepatology* **57**:461-469.
- 514 12. **Yu J, Li M, Wilkins J, Ding S, Swartz TH, Esposito AM, Zheng YM, Freed EO,
515 Liang C, Chen BK, Liu SL.** 2015. IFITM Proteins Restrict HIV-1 Infection by
516 Antagonizing the Envelope Glycoprotein. *Cell reports* **13**:145-156.
- 517 13. **Savidis G, Perreira JM, Portmann JM, Meraner P, Guo Z, Green S, Brass AL.** 2016.
518 The IFITMs Inhibit Zika Virus Replication. *Cell reports* **15**:2323-2330.
- 519 14. **Gorman MJ, Poddar S, Farzan M, Diamond MS.** 2016. The Interferon-Stimulated
520 Gene Ifitm3 Restricts West Nile Virus Infection and Pathogenesis. *J Virol* **90**:8212-8225.
- 521 15. **Poddar S, Hyde JL, Gorman MJ, Farzan M, Diamond MS.** 2016. The Interferon-
522 Stimulated Gene IFITM3 Restricts Infection and Pathogenesis of Arthritogenic and
523 Encephalitic Alphaviruses. *J Virol* **90**:8780-8794.

23

- 524 16. **Weiss SR, Navas-Martin S.** 2005. Coronavirus pathogenesis and the emerging pathogen
525 severe acute respiratory syndrome coronavirus. *Microbiol Mol Biol Rev* **69**:635-664.
- 526 17. **Zaki AM, van Boheemen S, Bestebroer TM, Osterhaus AD, Fouchier RA.** 2012.
527 Isolation of a novel coronavirus from a man with pneumonia in Saudi Arabia. *N Engl J*
528 *Med* **367**:1814-1820.
- 529 18. **Gaunt ER, Hardie A, Claas EC, Simmonds P, Templeton KE.** 2010. Epidemiology
530 and clinical presentations of the four human coronaviruses 229E, HKU1, NL63, and
531 OC43 detected over 3 years using a novel multiplex real-time PCR method. *Journal of*
532 *clinical microbiology* **48**:2940-2947.
- 533 19. **Dijkman R, Jebbink MF, Gaunt E, Rossen JW, Templeton KE, Kuijpers TW, van**
534 **der Hoek L.** 2012. The dominance of human coronavirus OC43 and NL63 infections in
535 infants. *J Clin Virol* **53**:135-139.
- 536 20. **Hilgenfeld R, Peiris M.** From SARS to MERS: 10 years of research on highly
537 pathogenic human coronaviruses. *Antiviral Res* **100**:286-295.
- 538 21. **Graham RL, Donaldson EF, Baric RS.** A decade after SARS: strategies for controlling
539 emerging coronaviruses. *Nat Rev Microbiol* **11**:836-848.
- 540 22. **Wrensch F, Winkler M, Pohlmann S.** IFITM proteins inhibit entry driven by the
541 MERS-coronavirus spike protein: evidence for cholesterol-independent mechanisms.
542 *Viruses* **6**:3683-3698.
- 543 23. **Bertram S, Dijkman R, Habjan M, Heurich A, Gierer S, Glowacka I, Welsch K,**
544 **Winkler M, Schneider H, Hofmann-Winkler H, Thiel V, Pohlmann S.** 2013.
545 TMPRSS2 activates the human coronavirus 229E for cathepsin-independent host cell
546 entry and is expressed in viral target cells in the respiratory epithelium. *J Virol* **87**:6150-
547 6160.
- 548 24. **John SP, Chin CR, Perreira J, Feeley EM, Aker A, Savidis G, Smith SE, Elia AE,**
549 **Everitt AR, Vora M, Pertel T, Elledge SJ, Kellam P, Brass AL.** 2013. The CD225
550 Domain of IFITM3 is Required for both IFITM Protein Association and Inhibition of
551 Influenza A Virus and Dengue Virus Replication. *J Virol*.
- 552 25. **Amini-Bavil-Olyaei S, Choi YJ, Lee JH, Shi M, Huang IC, Farzan M, Jung JU.**
553 2013. The antiviral effector IFITM3 disrupts intracellular cholesterol homeostasis to
554 block viral entry. *Cell Host Microbe* **13**:452-464.
- 555 26. **Li K, Markosyan RM, Zheng YM, Golfetto O, Bungart B, Li M, Ding S, He Y,**
556 **Liang C, Lee JC, Gratton E, Cohen FS, Liu SL.** 2013. IFITM proteins restrict viral
557 membrane hemifusion. *PLoS Pathog* **9**:e1003124.
- 558 27. **Desai TM, Marin M, Chin CR, Savidis G, Brass AL, Melikyan GB.** 2014. IFITM3
559 restricts influenza A virus entry by blocking the formation of fusion pores following
560 virus-endosome hemifusion. *PLoS Pathog* **10**:e1004048.
- 561 28. **Lin TY, Chin CR, Everitt AR, Clare S, Perreira JM, Savidis G, Aker AM, John SP,**
562 **Sarlah D, Carreira EM, Elledge SJ, Kellam P, Brass AL.** 2013. Amphotericin B
563 increases influenza A virus infection by preventing IFITM3-mediated restriction. *Cell*
564 *reports* **5**:895-908.
- 565 29. **Zhao X, Guo F, Liu F, Cuconati A, Chang J, Block TM, Guo JT.** 2014. Interferon
566 induction of IFITM proteins promotes infection by human coronavirus OC43. *Proc Natl*
567 *Acad Sci U S A* **111**:6756-6761.
- 568 30. **Lu J, Pan Q, Rong L, He W, Liu SL, Liang C.** 2011. The IFITM proteins inhibit HIV-
569 1 infection. *J Virol* **85**:2126-2137.

- 570 31. **Wrench F, Karsten CB, Gnirss K, Hoffmann M, Lu K, Takada A, Winkler M,**
571 **Simmons G, Pohlmann S.** 2015. Interferon-Induced Transmembrane Protein-Mediated
572 Inhibition of Host Cell Entry of Ebolaviruses. *J Infect Dis* **212 Suppl 2**:S210-218.
- 573 32. **Xie M, Xuan B, Shan J, Pan D, Sun Y, Shan Z, Zhang J, Yu D, Li B, Qian Z.** 2015.
574 Human cytomegalovirus exploits interferon-induced transmembrane proteins to facilitate
575 morphogenesis of the virion assembly compartment. *J Virol* **89**:3049-3061.
- 576 33. **Tandon R, Mocarski ES.** 2012. Viral and host control of cytomegalovirus maturation.
577 *Trends Microbiol* **20**:392-401.
- 578 34. **Li W, Moore MJ, Vasilieva N, Sui J, Wong SK, Berne MA, Somasundaran M,**
579 **Sullivan JL, Luzuriaga K, Greenough TC, Choe H, Farzan M.** 2003. Angiotensin-
580 converting enzyme 2 is a functional receptor for the SARS coronavirus. *Nature* **426**:450-
581 454.
- 582 35. **Everitt AR, Clare S, Pertel T, John SP, Wash RS, Smith SE, Chin CR, Feeley EM,**
583 **Sims JS, Adams DJ, Wise HM, Kane L, Goulding D, Digard P, Anttila V, Baillie JK,**
584 **Walsh TS, Hume DA, Palotie A, Xue Y, Colonna V, Tyler-Smith C, Dunning J,**
585 **Gordon SB, Gen II, Investigators M, Smyth RL, Openshaw PJ, Dougan G, Brass**
586 **AL, Kellam P.** 2012. IFITM3 restricts the morbidity and mortality associated with
587 influenza. *Nature* **484**:519-523.
- 588 36. **Bailey CC, Huang IC, Kam C, Farzan M.** 2012. Ifitm3 limits the severity of acute
589 influenza in mice. *PLoS Pathog* **8**:e1002909.
- 590 37. **Zhang YH, Zhao Y, Li N, Peng YC, Giannoulatou E, Jin RH, Yan HP, Wu H, Liu**
591 **JH, Liu N, Wang DY, Shu YL, Ho LP, Kellam P, McMichael A, Dong T.** 2013.
592 Interferon-induced transmembrane protein-3 genetic variant rs12252-C is associated with
593 severe influenza in Chinese individuals. *Nature communications* **4**:1418.
- 594 38. **Wang Z, Zhang A, Wan Y, Liu X, Qiu C, Xi X, Ren Y, Wang J, Dong Y, Bao M, Li**
595 **L, Zhou M, Yuan S, Sun J, Zhu Z, Chen L, Li Q, Zhang Z, Zhang X, Lu S, Doherty**
596 **PC, Kedzierska K, Xu J.** 2014. Early hypercytokinemia is associated with interferon-
597 induced transmembrane protein-3 dysfunction and predictive of fatal H7N9 infection.
598 *Proc Natl Acad Sci U S A* **111**:769-774.
- 599 39. **Jia R, Pan Q, Ding S, Rong L, Liu SL, Geng Y, Qiao W, Liang C.** 2012. The N-
600 terminal region of IFITM3 modulates its antiviral activity by regulating IFITM3 cellular
601 localization. *J Virol* **86**:13697-13707.
- 602 40. **Jia R, Xu F, Qian J, Yao Y, Miao C, Zheng YM, Liu SL, Guo F, Geng Y, Qiao W,**
603 **Liang C.** 2014. Identification of an endocytic signal essential for the antiviral action of
604 IFITM3. *Cell Microbiol* **16**:1080-1093.
- 605 41. **Compton AA, Roy N, Porrot F, Billet A, Casartelli N, Yount JS, Liang C, Schwartz**
606 **O.** 2016. Natural mutations in IFITM3 modulate post-translational regulation and toggle
607 antiviral specificity. *EMBO Rep* **17**:1657-1671.
- 608 42. **Chesarino NM, McMichael TM, Hach JC, Yount JS.** 2014. Phosphorylation of the
609 antiviral protein interferon-inducible transmembrane protein 3 (IFITM3) dually regulates
610 its endocytosis and ubiquitination. *J Biol Chem* **289**:11986-11992.
- 611 43. **Ganley IG, Carroll K, Bittova L, Pfeffer S.** 2004. Rab9 GTPase regulates late
612 endosome size and requires effector interaction for its stability. *Mol Biol Cell* **15**:5420-
613 5430.

- 614 44. **Yount JS, Karssemeijer RA, Hang HC.** 2012. S-palmitoylation and ubiquitination
615 differentially regulate interferon-induced transmembrane protein 3 (IFITM3)-mediated
616 resistance to influenza virus. *J Biol Chem* **287**:19631-19641.
- 617 45. **Yount JS, Moltedo B, Yang YY, Charron G, Moran TM, Lopez CB, Hang HC.** 2010.
618 Palmitoylome profiling reveals S-palmitoylation-dependent antiviral activity of IFITM3.
619 *Nat Chem Biol* **6**:610-614.
- 620 46. **Chesarino NM, McMichael TM, Yount JS.** 2015. E3 Ubiquitin Ligase NEDD4
621 Promotes Influenza Virus Infection by Decreasing Levels of the Antiviral Protein
622 IFITM3. *PLoS Pathog* **11**:e1005095.
- 623 47. **Chesarino NM, McMichael TM, Yount JS.** 2014. Regulation of the trafficking and
624 antiviral activity of IFITM3 by post-translational modifications. *Future Microbiol*
625 **9**:1151-1163.
- 626 48. **Lawe DC, Sitouah N, Hayes S, Chawla A, Virbasius JV, Tuft R, Fogarty K, Lifshitz
627 L, Lambright D, Corvera S.** 2003. Essential role of Ca²⁺/calmodulin in Early
628 Endosome Antigen-1 localization. *Mol Biol Cell* **14**:2935-2945.
- 629 49. **Hach JC, McMichael T, Chesarino NM, Yount JS.** 2013. Palmitoylation on conserved
630 and nonconserved cysteines of murine IFITM1 regulates its stability and anti-influenza A
631 virus activity. *J Virol* **87**:9923-9927.
- 632 50. **Warren CJ, Griffin LM, Little AS, Huang IC, Farzan M, Pyeon D.** 2014. The
633 antiviral restriction factors IFITM1, 2 and 3 do not inhibit infection of human
634 papillomavirus, cytomegalovirus and adenovirus. *PLoS One* **9**:e96579.
- 635 51. **Foster TL, Wilson H, Iyer SS, Coss K, Doores K, Smith S, Kellam P, Finzi A,
636 Borrow P, Hahn BH, Neil SJ.** 2016. Resistance of Transmitted Founder HIV-1 to
637 IFITM-Mediated Restriction. *Cell Host Microbe* **20**:429-442.
- 638 52. **Wu WL, Grotefend CR, Tsai MT, Wang YL, Radic V, Eoh H, Huang IC.** 2017.
639 Delta20 IFITM2 differentially restricts X4 and R5 HIV-1. *Proc Natl Acad Sci U S A*
640 **114**:7112-7117.
- 641 53. **Fu B, Wang L, Li S, Dorf ME.** 2017. ZMPSTE24 defends against influenza and other
642 pathogenic viruses. *J Exp Med* **214**:919-929.
- 643 54. **Gerlach T, Hensen L, Matrosovich T, Bergmann J, Winkler M, Peteranderl C,
644 Klenk HD, Weber F, Herold S, Pohlmann S, Matrosovich M.** 2017. pH Optimum of
645 Hemagglutinin-Mediated Membrane Fusion Determines Sensitivity of Influenza A
646 Viruses to the Interferon-Induced Antiviral State and IFITMs. *J Virol* **91**.
- 647 55. **Desai TM, Marin M, Mason C, Melikyan GB.** 2017. pH regulation in early endosomes
648 and interferon-inducible transmembrane proteins control avian retrovirus fusion. *J Biol
649 Chem* **292**:7817-7827.
- 650 56. **Rabbani MA, Ribaldo M, Guo JT, Barik S.** 2016. Identification of IFN-stimulated
651 gene (ISG) proteins that inhibit human parainfluenza virus type 3. *J Virol*.
- 652 57. **Yount JS, Zhang MM, Hang HC.** 2013. Emerging roles for protein S-palmitoylation in
653 immunity from chemical proteomics. *Current opinion in chemical biology* **17**:27-33.
- 654 58. **Jia R, Ding S, Pan Q, Liu SL, Qiao W, Liang C.** 2015. The C-terminal sequence of
655 IFITM1 regulates its anti-HIV-1 activity. *PLoS One* **10**:e0118794.
- 656 59. **Li K, Jia R, Li M, Zheng YM, Miao C, Yao Y, Ji HL, Geng Y, Qiao W, Albritton
657 LM, Liang C, Liu SL.** 2015. A sorting signal suppresses IFITM1 restriction of viral
658 entry. *J Biol Chem* **290**:4248-4259.

- 659 60. **Jiang D, Guo H, Xu C, Chang J, Gu B, Wang L, Block TM, Guo JT.** 2008.
660 Identification of three interferon-inducible cellular enzymes that inhibit the replication of
661 hepatitis C virus. *J Virol* **82**:1665-1678.
- 662 61. **Weidner JM, Jiang D, Pan XB, Chang J, Block TM, Guo JT.** 2010. Interferon-
663 induced cell membrane proteins, IFITM3 and tetherin, inhibit vesicular stomatitis virus
664 infection via distinct mechanisms. *J Virol* **84**:12646-12657.
- 665 62. **Chang J, Warren TK, Zhao X, Gill T, Guo F, Wang L, Comunale MA, Du Y, Alonzi
666 DS, Yu W, Ye H, Liu F, Guo JT, Mehta A, Cuconati A, Butters TD, Bavari S, Xu X,
667 Block TM.** 2013. Small molecule inhibitors of ER alpha-glucosidases are active against
668 multiple hemorrhagic fever viruses. *Antiviral Res.*
- 669 63. **Lin HX, Feng Y, Tu X, Zhao X, Hsieh CH, Griffin L, Junop M, Zhang C.** 2011.
670 Characterization of the spike protein of human coronavirus NL63 in receptor binding and
671 pseudotype virus entry. *Virus Res* **160**:283-293.
- 672 64. **He J, Choe S, Walker R, Di Marzio P, Morgan DO, Landau NR.** 1995. Human
673 immunodeficiency virus type 1 viral protein R (Vpr) arrests cells in the G2 phase of the
674 cell cycle by inhibiting p34cdc2 activity. *J Virol* **69**:6705-6711.
- 675 65. **Connor RI, Chen BK, Choe S, Landau NR.** 1995. Vpr is required for efficient
676 replication of human immunodeficiency virus type-1 in mononuclear phagocytes.
677 *Virology* **206**:935-944.
- 678 66. **Zhao X, Guo F, Comunale MA, Mehta A, Sehgal M, Jain P, Cuconati A, Lin H,
679 Block TM, Chang J, Guo JT.** 2015. Inhibition of endoplasmic reticulum-resident
680 glucosidases impairs severe acute respiratory syndrome coronavirus and human
681 coronavirus NL63 spike protein-mediated entry by altering the glycan processing of
682 angiotensin I-converting enzyme 2. *Antimicrob Agents Chemother* **59**:206-216.
- 683 67. **Chang J, Warren TK, Zhao X, Gill T, Guo F, Wang L, Comunale MA, Du Y, Alonzi
684 DS, Yu W, Ye H, Liu F, Guo JT, Mehta A, Cuconati A, Butters TD, Bavari S, Xu X,
685 Block TM.** 2013. Small molecule inhibitors of ER alpha-glucosidases are active against
686 multiple hemorrhagic fever viruses. *Antiviral Res* **98**:432-440.
- 687 68. **Milewska A, Zarebski M, Nowak P, Stozek K, Potempa J, Pyrc K.** 2014. Human
688 coronavirus NL63 utilizes heparan sulfate proteoglycans for attachment to target cells. *J
689 Virol* **88**:13221-13230.
690

691 **FIGURE LEGENDS**

692

693 **Fig. 1 IFITM proteins inhibit the infection of pseudoviruses in FLIP-IN T REX 293 and**694 **Huh7.5 cells. (A)** The expression of FLAG-tagged IFITMs in FLIP-IN T Rex 293 cells cultured

695 in the presence of 1µg/ml of tetracycline (tet) for 24 h and in Huh7.5-derived stable cell lines

696 was detected by a Western blot assay using a monoclonal antibody against Flag tag. β-actin

697 served as a loading control. **(B)** FLIP-IN T Rex 293 cells expressing chloramphenicol

698 acetyltransferase (CAT) or the indicated IFITM protein were cultured in the presence or absence

699 of tet for 24 h and then infected with 229Epp, NL63pp, SARSpp, MERSpp, IAVpp, or LASVpp.

700 Luciferase activities were determined at 48 h post infection (hpi). Relative infection efficiency is

701 the ratio of luciferase activity in cells cultured in the presence of tet over that in cells cultured in

702 the absence of tet. Error bars indicate standard deviations (n = 6). IFITMs do not significantly

703 affect the infection of LASVpp, but significantly ($p < 0.001$) inhibit the infection of all other704 tested pseudotyped viruses. **(C)** Huh7.5 cells expressing N-terminally FLAG-tagged human

705 IFITM proteins or transduced with empty vector (pQCXIP) were infected with indicated

706 pseudoviruses. Luciferase activities were determined at 48 hpi. Relative infection is the ratio of

707 luciferase activity of cells expressing the indicated IFITM protein over that of cells transduced

708 with empty vector. Error bars indicate standard deviations (n = 6). All three IFITM proteins

709 significantly ($p < 0.001$) inhibited the infection of all the pseudoviruses, except for LASVpp.

710

711 **Fig. 2 Y20 of IFITM3 plays a critical role in modulating the entry of 229E, MERS-CoV**712 **SARS-CoV and NL63 in both 293 and Huh7.5 cells. (A)** FLIP-IN T Rex cells expressing CAT

713 or the indicated wild-type or mutant IFITM proteins were cultured in the presence of 1 μ g/ml of
714 tet for 24 h. Expression of FLAG-tagged IFITM mutants was detected by Western blot assay
715 using anti-Flag monoclonal antibody. β -actin served as a loading control. **(B to E)** The above
716 FLP-IN T Rex-derived cell lines were cultured in the presence or absence of tet for 24 h and then
717 infected with HCoV-OC43pp (B), SARSpp or NL63pp (C), 229Epp (D) MERSpp and LASVpp
718 (E). Luciferase activities were determined at 48 hpi. Relative infection efficiency is the ratio of
719 luciferase activity in cells cultured in the presence of tet over that in cells cultured in the absence
720 of tet. Error bars indicate standard deviations (n = 6). **(F)** Huh7.5 cells were stably transduced
721 with empty retroviral vector (pQCXIP) or vectors expressing wild-type or mutant IFITM3
722 proteins. Expression of FLAG-tagged IFITM proteins was detected by Western blot assay using
723 anti-Flag monoclonal antibody. β -actin served as a loading control. **(G to K)** The above Huh7.5-
724 derived cell lines were infected with OC43pp **(G)**, SARSpp and NL63pp (H), 229Epp (I),
725 MERSpp (J) or LASVpp (K). Luciferase activities were determined at 48 hpi. Relative infection
726 is the ratio of luciferase activity of cells expressing the indicated IFITM protein over that of cells
727 transduced with empty vector. Error bars indicate standard deviations (n = 6).

728

729 **Fig. 3 Y20 mutation alters IFITM3 subcellular localization.** FLP-IN T Rex cells expressing
730 the indicated wild-type and mutant IFITM3 proteins were cultured in the presence of tet for 24 h
731 to induce the IFITM expression. The localization of FLAG-tagged IFITM3 **(A)**, IFITM3/Y20A
732 **(B)** and IFITM3/Y20D **(C)** was detected by immunofluorescent staining with an anti-Flag
733 monoclonal antibody (red). EEA1, Rab5 or Rab9 were visualized by immunofluorescent staining
734 with respective antibodies (green). Cell nuclei were stained with DAPI (Blue).

735

736 **Fig. 4 IFITM3/Y20A-enhanced SARSpp and MERSpp infection is low pH dependent. (A)**

737 Huh7.5 cells were infected with OC43pp, MERSpp, SARSpp, NL63pp, or 229Epp in the

738 absence (mock) or presence of indicated concentrations of NH₄Cl. Luciferase activities were

739 determined at 48 hpi. Relative infection is the ratio of luciferase activity in cells treated with

740 NH₄Cl over that in the mock-treated cells. Error bars indicate standard deviations (n = 6). **(B**

741 **and C)** Huh7.5 cells stably expressing indicated wild-type or Y20A mutant IFITM3 proteins or

742 transduced with empty vector were infected with MERSpp (B) or SARSpp (C) in the absence

743 (mock) or presence of indicated concentrations of NH₄Cl. Luciferase activities were determined

744 at 48 hpi. Relative infection is the ratio of luciferase activity in cells treated with NH₄Cl over

745 that in the mock-treated cells. Error bars indicate standard deviations (n = 6).

746

747 **Fig. 5 Y99 of IFITM3 plays a critical role in modulating the entry of HCoV** (A) FLIP-IN T

748 Rex 293 cells expressing CAT, IFITM3, or indicated mutant IFITM3 proteins were cultured in

749 the presence of 1 μg/ml of tet for 24 h. Expression of FLAG-tagged IFITM proteins was detected

750 by Western blot assay using anti-Flag monoclonal antibody. β-actin served as a loading control.

751 **(B to F)** FLP-IN T Rex 293-derived cells were cultured in the presence of tet for 24 h to induce

752 the IFITM mutant expression. Cells were then infected with HCoV-OC43pp (B), SARSpp or

753 NL63pp (C), 229Epp (D), VSVpp or IAVpp (E), and MERSpp(F), respectively. Luciferase

754 activities were determined at 48 hpi. Relative infection efficiency represents luciferase activity of

755 cells cultured with tet normalized to that of cells cultured in the absence of tet. Error bars

756 indicate standard deviations (n = 6).

757

758 **Fig. 6 Palmitoylation, ubiquitination and oligomerization are important for IFITM3**
759 **restriction of HCoV entry.** (A) FLIP-IN T Rex 293 cells expressing CAT or the indicated wild-
760 type and mutant IFITM3 proteins were cultured in the presence of tet for 24 h. Expression of the
761 IFITM proteins was detected by Western blot assay using anti-Flag monoclonal antibody. β -actin
762 served as a loading control. (B) The above FLP-IN T Rex-derived cells were cultured in the
763 presence or absence of tet for 24 h and then infected with SARSpp, NL63pp, 229Epp, MERSpp,
764 IAVpp, or MLVpp. Luciferase activities were determined at 48 hpi. Relative infection efficiency
765 is the ratio of luciferase activity in cells cultured in the presence of tet over that in cells cultured
766 in the absence of tet. Error bars indicate standard deviations ($n = 6$).

767

768 **Fig. 7 Role of the IFITM1 C-terminal motifs in modulating the entry of HCoVs.** (A) FLIP-
769 IN T Rex cells expressing CAT, wild-type or mutant IFITM1 proteins were cultured in the
770 presence of tet for 24 h. Expression of FLAG-tagged IFITM1 proteins was detected by
771 Western blot assay using anti-Flag monoclonal antibody. β -actin served as a loading control. (B
772 to D) The above cell lines were left untreated or treated with $1\mu\text{g/ml}$ of tet for 24 h to induce the
773 IFITM expression. Cells were then infected with SARSpp, NL63pp, or MLVpp (B), 229Epp (C),
774 or MERSpp (D). Luciferase activities were determined at 48 hpi. Relative infection efficiency is
775 the ratio of luciferase activity in cells cultured in the presence of tetracycline over that in cells
776 cultured in the absence of tetracycline. Error bars indicate standard deviations ($n = 6$). **
777 compared to wild-type IFITM1, $p < 0.001$.

778

779 **Fig. 8 Role of the IFITM1 C-terminal motifs in modulating the infection of HCoV-NL63 in**
780 **Huh7.5 cells.** (A) Huh7.5 cells were stably transduced with retroviral vectors expressing wild-

781 type IFITM1, IFITM1/TC6, IFITM1/TC18 or empty vector (pQCXIP). Expression of FLAG-
782 tagged IFITM1 proteins was detected by Western blot assay using anti-Flag monoclonal
783 antibody. β -actin served as a loading control. **(B)** The above cell lines were infected with
784 SARSpp, NL63pp or MLVpp. Luciferase activities were determined at 48 hpi. Relative
785 infection is the ratio of luciferase activity of cells expressing the indicated IFITM protein over
786 that of cells transduced with empty vector. Error bars indicate standard deviations ($n = 6$). **(C)**
787 The above cell lines were infected with HCoV-NL63 virus at a M.O.I. of 5. Infected cells were
788 visualized immunofluorescent staining using NL63 NP monoclonal antibody (green). Cell nuclei
789 were stained with DAPI (blue). Percentages of cells infected by NL63 were expressed as average
790 \pm standard deviation. **(D)** The amounts of intracellular HCoV-NL63 RNA at 24 hpi were
791 quantified by a qRT-PCR assay and expressed as the ratio of viral RNA in IFITM-expressing
792 cells over that in the cells transduced with empty vector. Error bars indicate standard deviations
793 ($n = 4$).

794

795 **Figure 9. Subcellular localization of wild-type and C-terminally truncated IFITM1 proteins.**

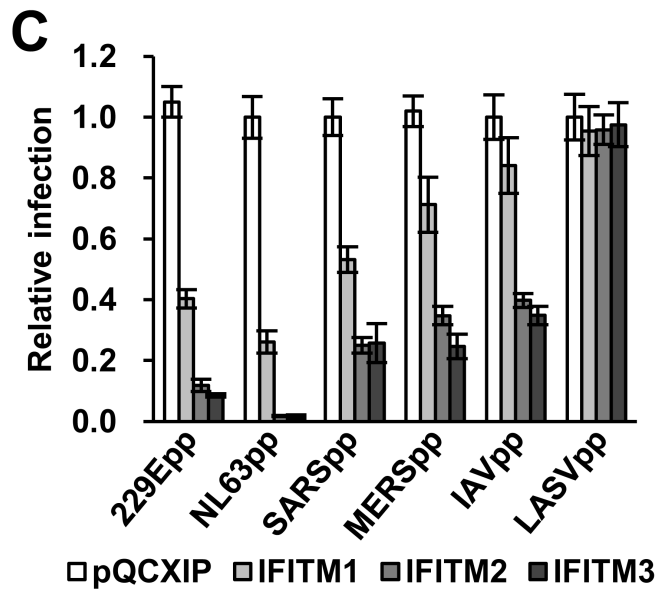
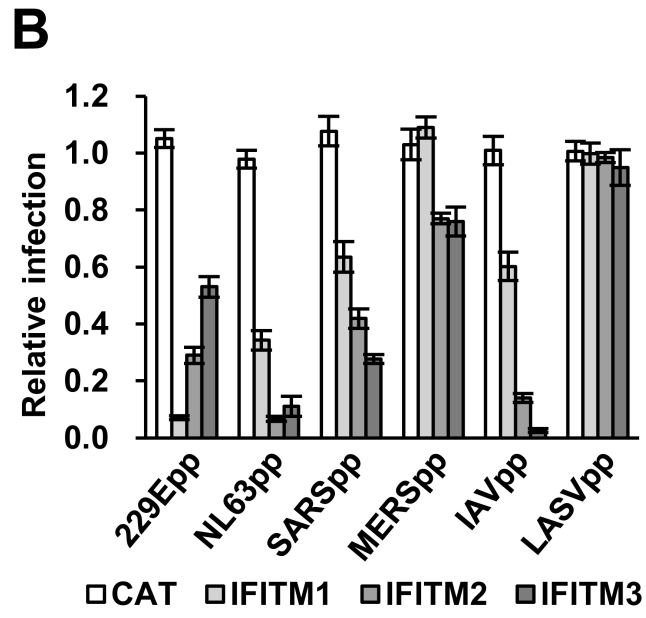
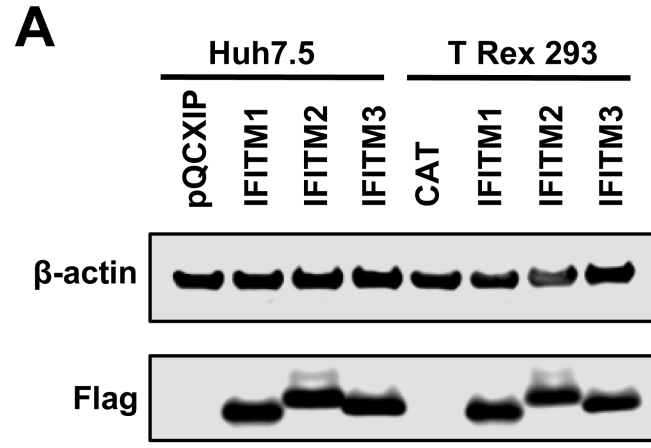
796 FLP-IN T Rex 293 cells expressing the indicated wild-type and mutant IFITM1 proteins were
797 treated with $1\mu\text{g/ml}$ of tetracycline for 24 h to induce the IFITM expression. The localization of
798 FLAG-tagged IFITM1 **(A)**, IFITM1/TC6 **(B)** and IFITM1/TC18 **(C)** was detected by
799 immunofluorescent staining with an anti-Flag monoclonal antibody (red). EEA1, Rab5 or Rab9
800 were visualized by immunofluorescent staining with respective antibodies (green). Cell nuclei
801 were stained with DAPI (Blue).

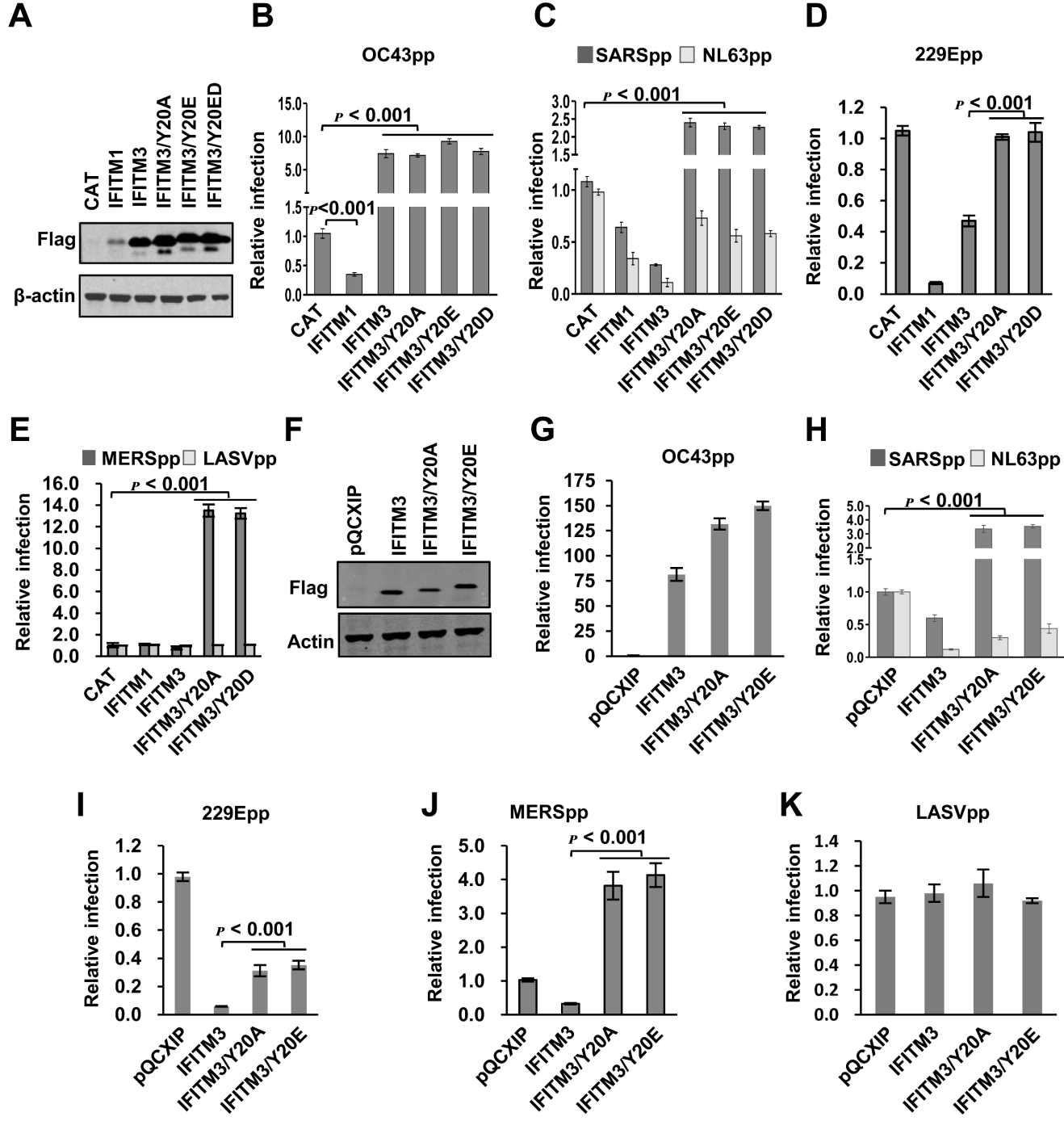
802

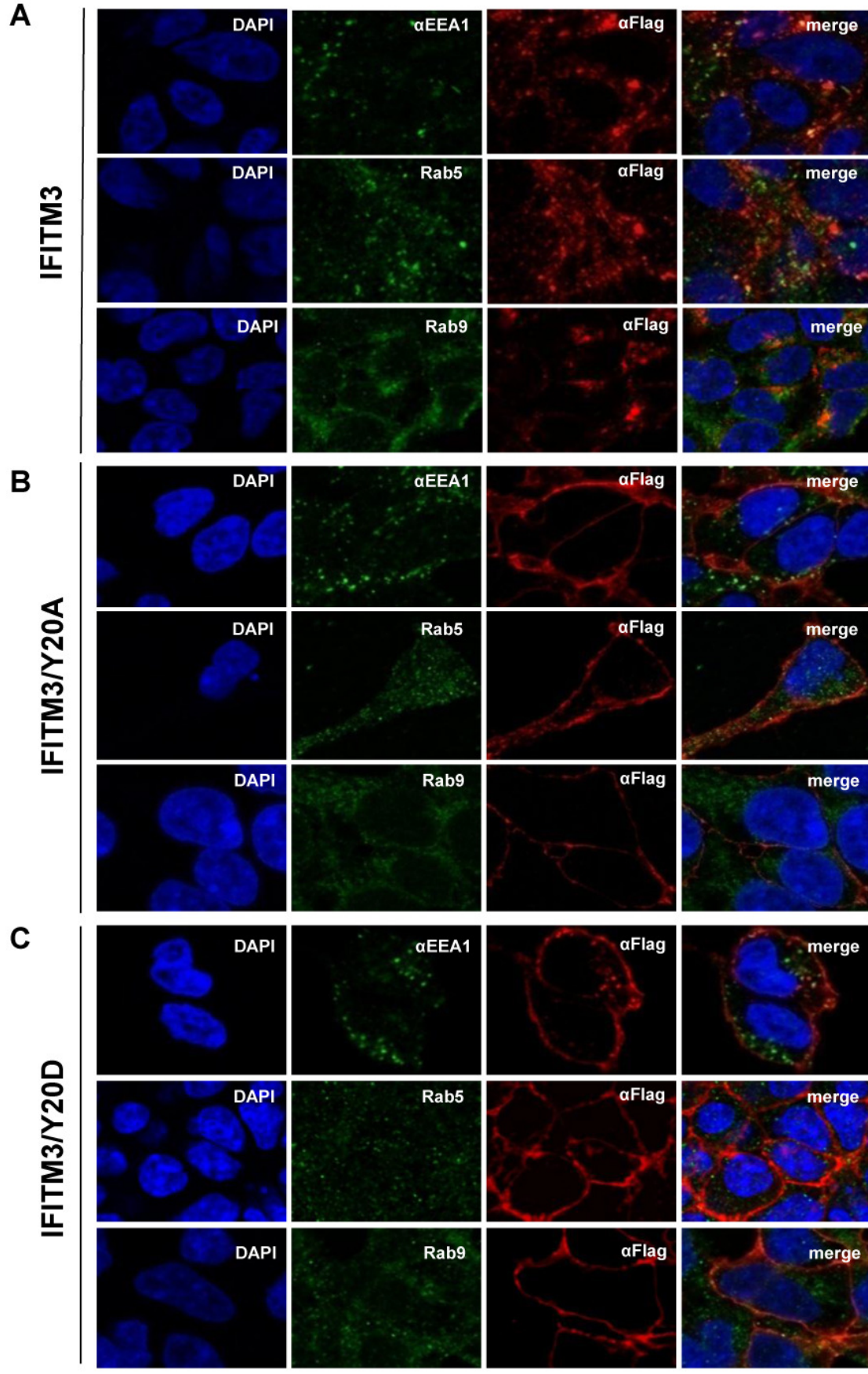
803 **Figure 10. C-terminal motif of IFITM1 is required for its ubiquitination.** 293T cells were
804 transfected with a plasmid expressing the indicated FLAG-tagged wild-type and mutant IFITM1
805 or IFITM3 proteins. Immunoprecipitation was performed by using an anti-FLAG monoclonal
806 antibody. The precipitated proteins were resolved by SDS-PAGE and blotted onto a membrane.
807 IFITM proteins and their ubiquitinated species were visualized by probing with an anti-FLAG
808 rabbit polyclonal antibody (**A**) or anti-ubiquitin rabbit polyclonal antibody (**B**). The mono-
809 ubiquitinated and di-ubiquitinated form of IFITM were indicated by a single- and double-
810 asterisk, respectively. IFITM proteins without ubiquitination with the molecular weight smaller
811 than 15kDa serve as loading controls.

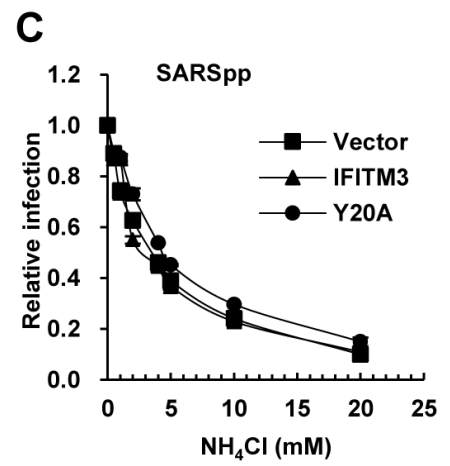
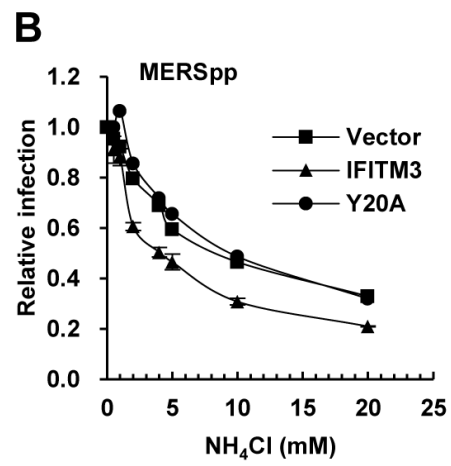
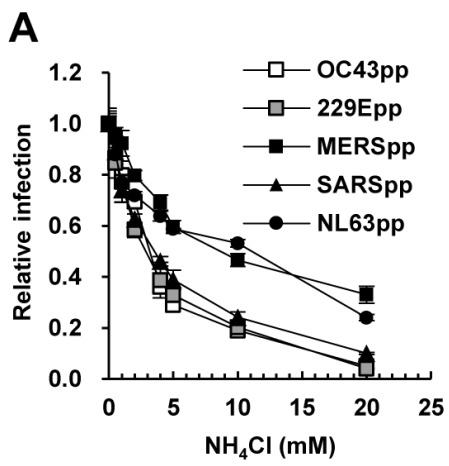
812

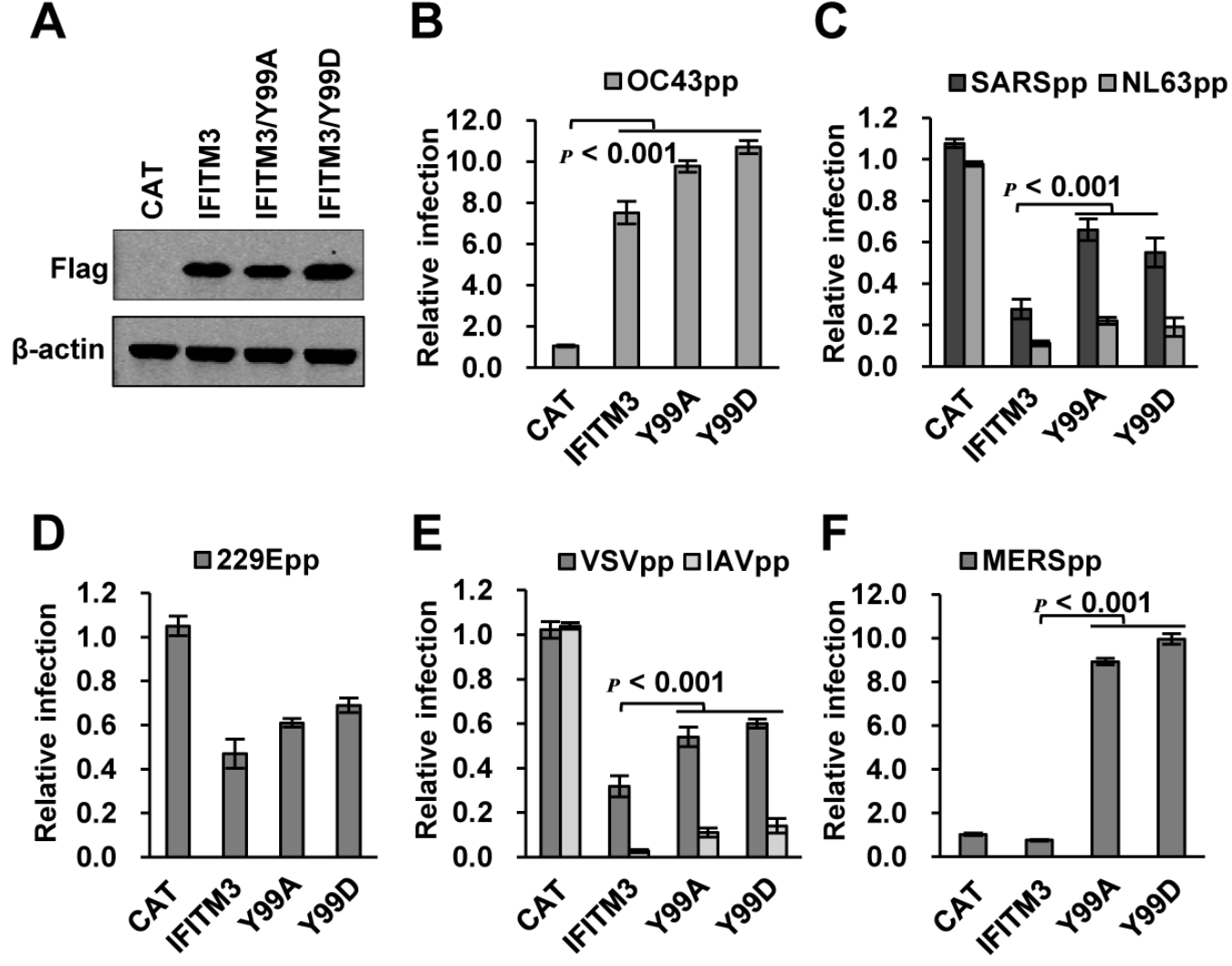
813 **Figure 11. Illustration of IFITM protein structural domains and motifs important for**
814 **subcellular trafficking, oligomerization and post-translational modification.** An alignment
815 of human IFITM1, IFITM2 and IFITM3 protein sequence by using Vector NTI 8.0 software is
816 shown. Five structural domains including N-terminal domain (NTD), intramembrane domain
817 (IMD), intracellular loop (CIL), transmembrane domain (TMD), and C-terminal domain (CTD)
818 are indicated. IMD and CIL domains comprise the canonical CD225 domain (shown in red).
819 ²⁰YXXΦ²³ motif required for IFITM3 endocytosis and ¹²²KRXX¹²⁵ motif that serves as a sorting
820 signal for IFITM1 are underlined with purple lines. The putative phosphorylation, palmitoylation
821 and ubiquitination sites are indicated. Two phenylalanine residues in the IMD that promote
822 IFITM oligomerization are indicated with red up-triangles.

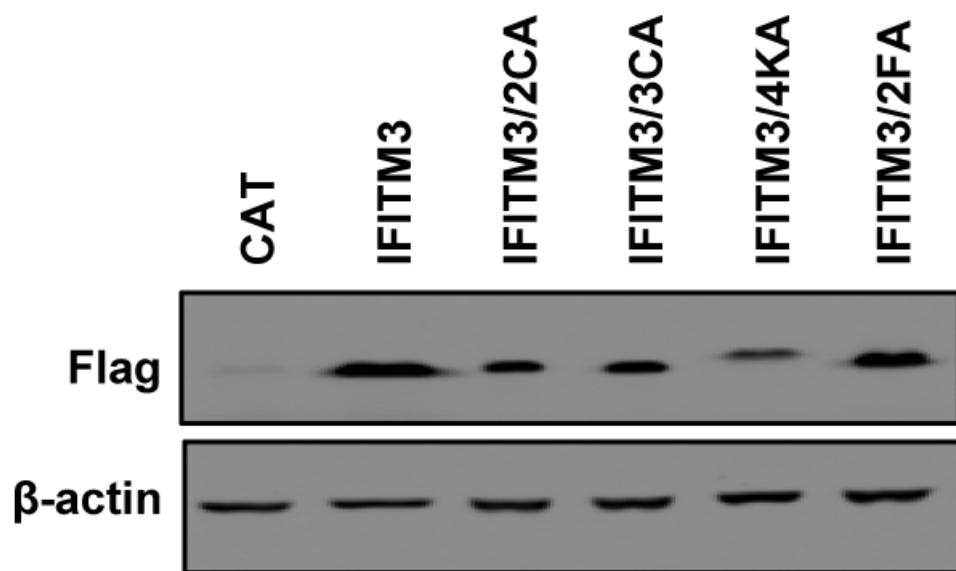
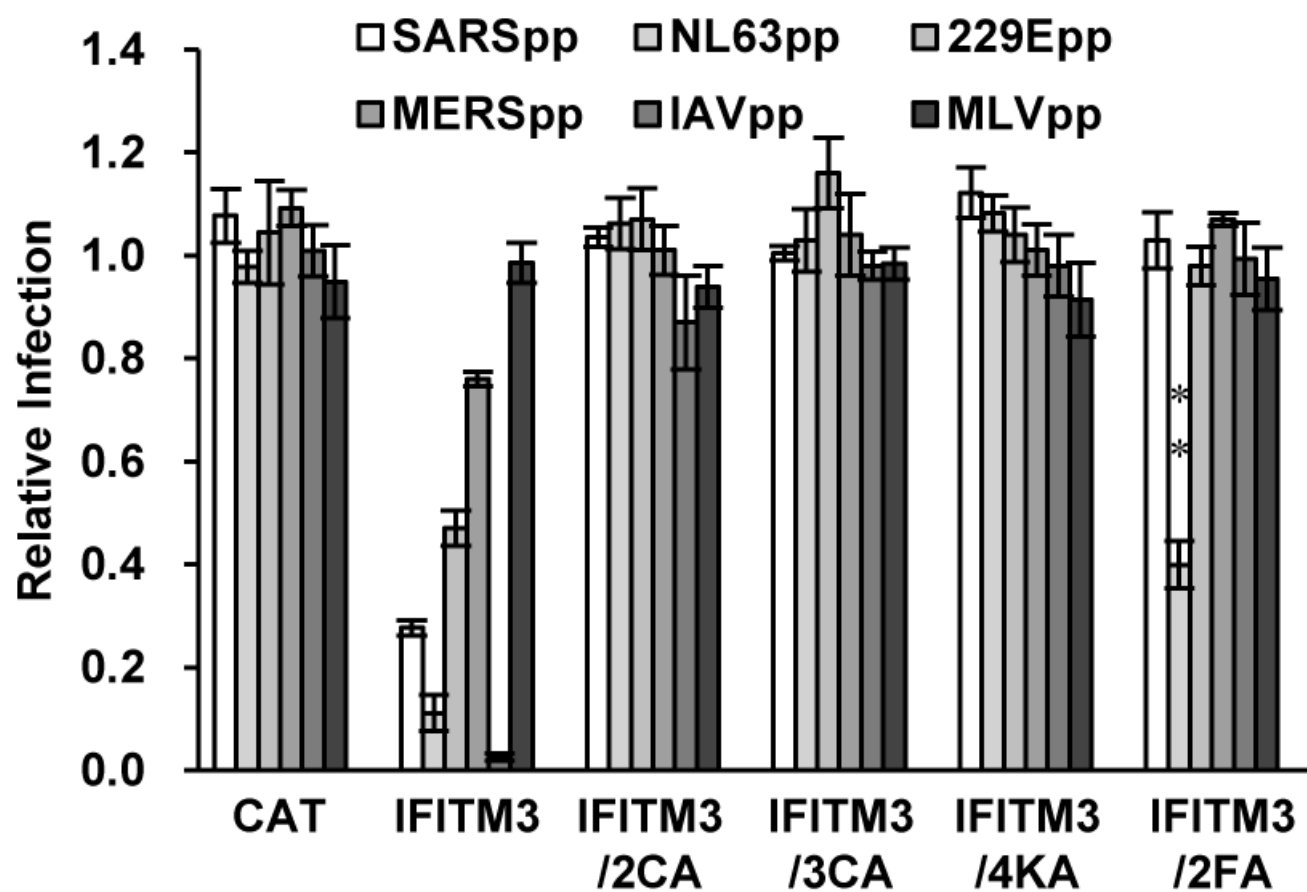


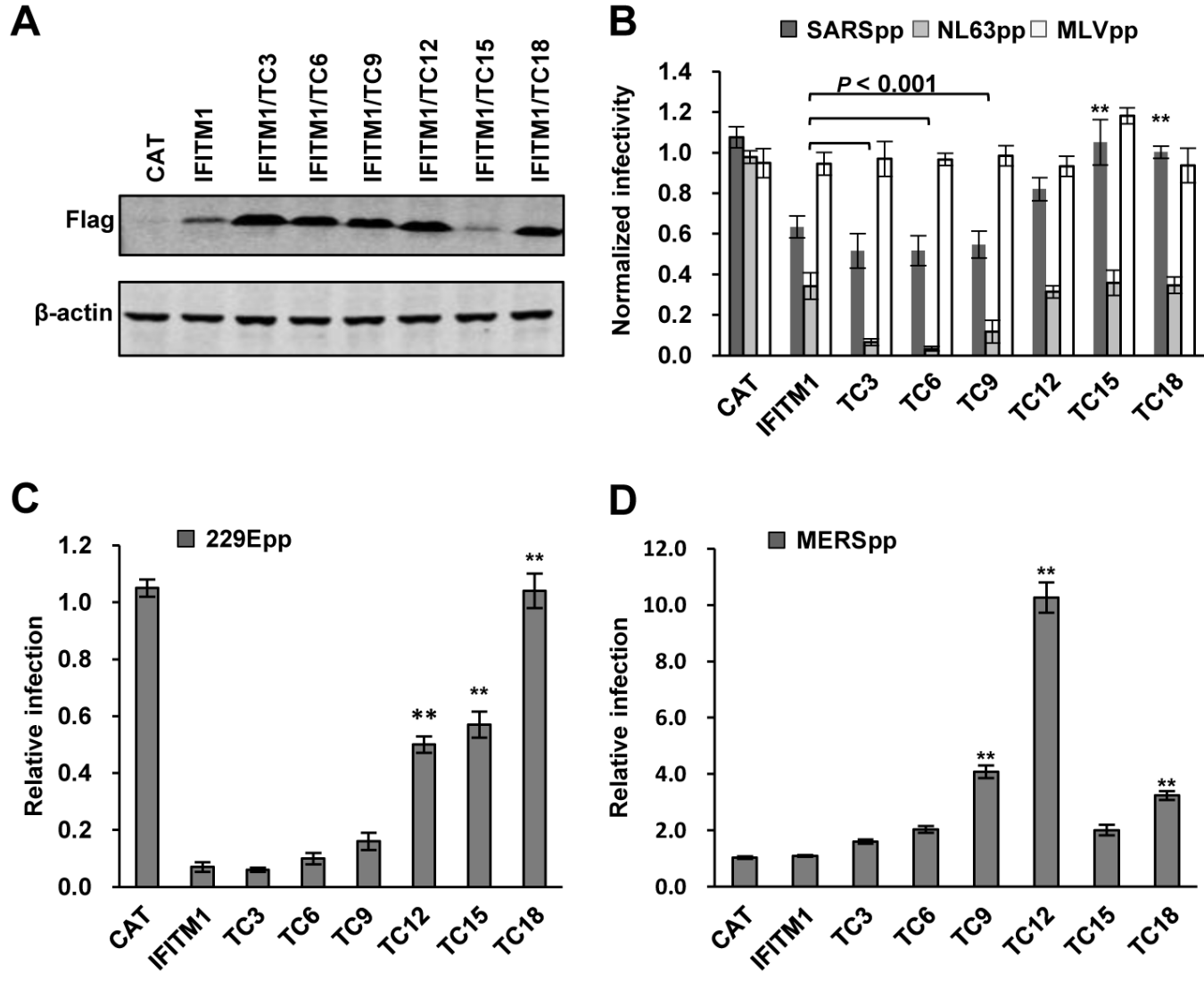


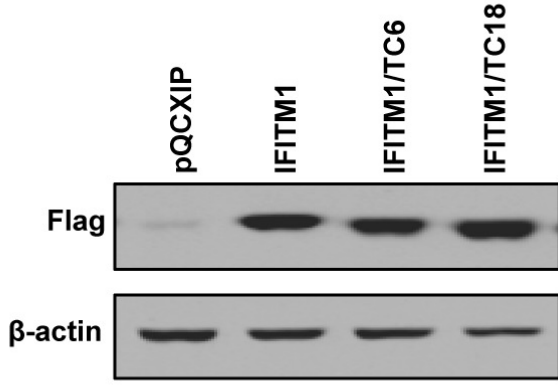
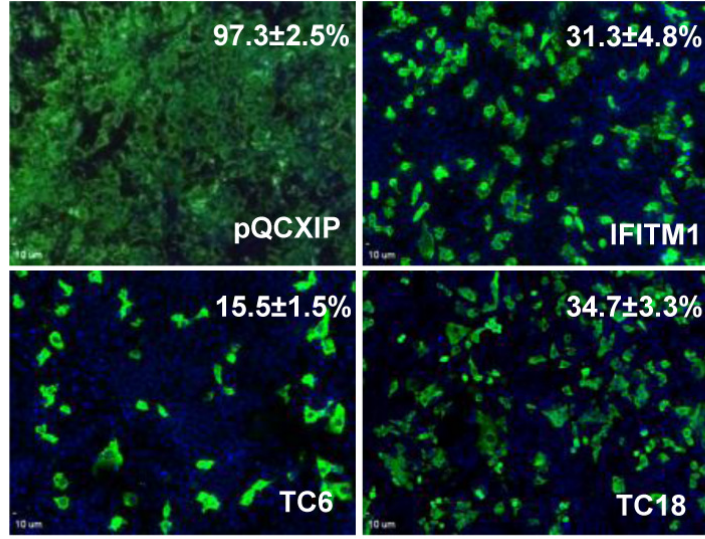
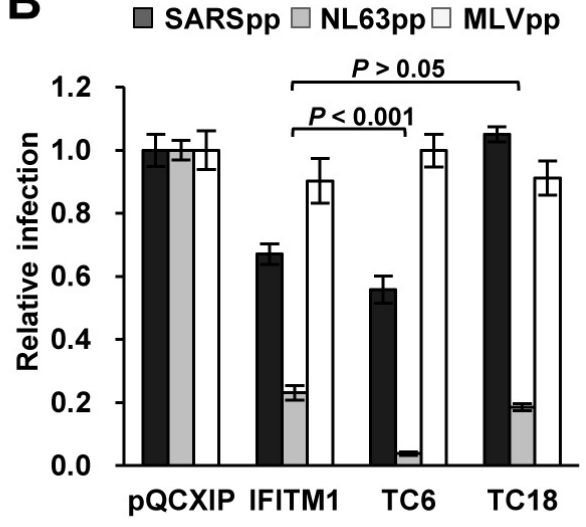






A**B**



A**C****B****D**